Nat Hazards (2008) 45:211–233
DOI 10.1007/s11069-007-9161-y

ORIGINAL PAPER

Quantitative sinkhole hazard assessment. A case study from the Ebro Valley evaporite alluvial karst (NE Spain)

Francisco Gutiérrez · Jesús Guerrero · Pedro Lucha

Received: 2 January 2006 / Accepted: 25 October 2006 / Published online: 26 February 2008
© Springer Science+Business Media B.V. 2008

Abstract Quantitative sinkhole hazard assessments in karst areas allow calculation of the potential sinkhole risk and the performance of cost-benefit analyses. These estimations are of practical interest for planning, engineering, and insurance purposes. The sinkhole hazard assessments should include two components: the probability of occurrence of sinkholes (sinkholes/km^2 year) and the severity of the sinkholes, which mainly refers to the subsidence mechanisms (progressive passive bending or catastrophic collapse) and the size of the sinkholes at the time of formation; a critical engineering design parameter. This requires the compilation of an exhaustive database on recent sinkholes, including information on the: (1) location, (2) chronology (precise date or age range), (3) size, and (4) subsidence mechanisms and rate. This work presents a hazard assessment from an alluvial evaporite karst area (0.81 km^2) located in the periphery of the city of Zaragoza (Ebro River valley, NE Spain). Five sinkholes and four locations with features attributable to karstic subsidence where identified in an initial investigation phase providing a preliminary probability of occurrence of 0.14 sinkholes/km^2 year (11.34% in annual probability). A trenching program conducted in a subsequent investigation phase allowed us to rule out the four probable sinkholes, reducing the probability of occurrence to 0.079 sinkholes/km^2 year (6.4% in annual probability). The information on the severity indicates that collapse sinkholes 10–15 m in diameter may occur in the area. A detailed study of the deposits and deformational structures exposed by trenching in one of the sinkholes allowed us to infer a modern collapse sinkhole approximately 12 m in diameter and with a vertical throw of 8 m. This collapse structure is superimposed on a subsidence sinkhole around 80 m across that records at least 1.7 m of synsedimentary subsidence. Trenching, in combination with dating techniques, is proposed as a useful methodology to elucidate the origin of depressions with uncertain diagnosis and to gather practical information with predictive utility about particular sinkholes in alluvial karst settings: precise location, subsidence mechanisms and magnitude, and timing and rate of the subsidence episodes.

F. Gutiérrez (✉) · J. Guerrero · P. Lucha
Department of Earth Sciences, University of Zaragoza,
Edificio Geológicas, C/. Pedro Cerbuna 12, 50009 Zaragoza, Spain
e-mail: fgutier@unizar.es

Keywords Sinkhole hazard assessment · Probability of occurrence · Severity · Trenching · Evaporite karst · Ebro Basin

1 Introduction

The damage derived from the generation of new sinkholes and the activity or reactivation of previously existing ones have a significant detrimental effect on the economy and the social welfare of numerous regions (Martínez et al. 1998; Waltham et al. 2005). As examples, the direct economic losses caused by the single collapse events related to the karstification of tertiary evaporites that occurred in 1998 and 2003 in the Spanish cities of Oviedo and Calatayud were estimated at 18 and 4.8 million euros, respectively (M. Gutiérrez-Claverol pers. comm. and Gutiérrez et al. 2004a). Additionally, collapse sinkholes formed in a catastrophic way may also endanger human lives. In 1962 and 1964, collapse sinkholes triggered by groundwater abstraction for gold mining in the dolomite karst of the Far West Rand (Transvaal, South Africa) engulfed several buildings with the loss of 29 and 5 lives, respectively (Bezuidenhout and Enslin 1970). However, in most karst areas the sinkhole risk remains unknown or underestimated partly due to several aspects related to the inherent nature of this geological phenomenon: (1) commonly, the total subsidence damage in a given karst area is not due to a few easily identifiable disastrous subsidence events but to a large number of high-frequency and regular-sized sinkholes with a limited impact; (2) the indirect damage caused by sinkholes (e.g., reduction in property value or economic production) may be larger than the direct losses and difficult to identify and quantify; (3) subsidence damaging events are frequently hidden by the affected landowners to avoid depreciation of their property. In spite of these difficulties, attempts should be made to assess the sinkhole risk in retrospective and prospective ways.

The potential annual sinkhole risk in a given area may be estimated by applying the widely used formula (Bell 1999; Crozier and Glade 2004):

$$R = \sum H\,E\,V$$

where R is the risk expressed in terms of victims/year or monetary value/year, H is the hazard, E is the exposure or elements at risk, referring to the number of persons and the economic value of the properties that may be affected by subsidence, and V is the vulnerability, or the unitary fraction of the exposure that is expected to be damaged if affected by a sinkhole. The total risk will correspond to the sum of the estimated risk for each exposed human element. Preferably, the hazard should include two components: the probability of occurrence of sinkholes (number of sinkholes/km^2 year or number of sinkholes/year in the considered area) (Beck 1991) and the severity of the sinkholes (Ayala-Carcedo 2002). The severity refers to the attributes of the sinkholes and the processes involved in their generation that determine their capability to cause damage: mainly the size at the time of formation and the subsidence rate, which is largely dependent on the subsidence mechanism (catastrophic collapse or progressive passive bending). The initial diameter of the sinkholes is a crucial engineering design parameter (Jones and Cooper 2005). In an ideal situation we should tend to produce, like with other hazardous geological processes (floods, earthquakes), scaling relationships between the magnitude and frequency of sinkholes.

As is widely accepted, an effective risk-mitigation program should include three complementary types of activities (Smith 1996; Cendrero 1997): (1) scientific and technical studies (e.g., hazard assessment, design and application of mitigation measures); (2) educational programs mainly focused on ensuring perception of the risk among the population and decision makers; and (3) political and administrative tasks which should include decisions oriented to prevent or reduce the damage (land-use planning, regulations). Obviously, the scientific and technical work, although indispensable to accomplish a satisfactory mitigation program, is insufficient and even useless if it is not followed by consequent political decisions (Cendrero 1997). Unfortunately, in many cases political and administrative involvement is insufficient or inadequate. One of the many underlying reasons for this could be that often, we, the scientists and consultants, do not communicate the problem well enough to generate a competent reaction from the administration. The sinkhole hazard is frequently presented in a qualitative and descriptive fashion and in many cases expressed graphically through unvalidated susceptibility maps with an unknown reliability or predictive capability (Remondo et al. 2003; Gutiérrez-Santolalla et al. 2005a). Probably, one of the most effective ways to raise perception and awareness amongst decision makers would be providing rough estimates of the sinkhole risk in terms of potential annual economic losses and victims. This task, which may be also useful for insurance and engineering purposes, requires the quantification of the sinkhole hazard.

Sinkhole hazard assessments should be based on thorough studies of recent sinkhole activity. The following aspects should be addressed: (1) the spatial distribution of the sinkholes; (2) the chronology of the sinkholes; (3) the size of the sinkholes at the time of formation; and (4) the activity and evolution of the sinkholes (subsidence rate and mechanisms, reactivations, enlargement, etc.). The first two of these aspects allow us to estimate the probability of occurrence of sinkholes (number of sinkholes/km^2 year) (Beck 1991), whereas the last two provide information on the severity of the phenomenon. It is important to note that, if no chronological information is available, the probability of occurrence of sinkholes cannot be estimated. A higher sinkhole density does not necessarily means a higher probability of occurrence. In most cases we are not able to identify all of the sinkholes formed in the past, and consequently, we end up with a minimum or optimistic estimation of the spatio-temporal frequency of sinkholes. Obviously, the reliability of our predictions will depend on the quantity (completeness) and quality of the available data. The probability of occurrence indicates how many sinkholes may form in a given area during a certain time span or the annual probability of sinkhole formation, but not where and when the sinkholes will occur. The investigation on the aspects related to the severity of old sinkholes might allow us to foresee how the future and existing sinkholes may form and/or evolve. These predictions are based on the assumption that future sinkholes will have a similar behavior to the sinkholes formed in the past (Principle of Uniformitarianism). However, this hypothesis may not be valid and the subsidence phenomena may show a different degree of activity in the future. For this reason, it would be desirable to analyze whether the factors that control the dissolution and subsidence processes may undergo changes during the time considered in our predictions and if those natural or human-induced variations may have a positive (attenuating) or negative (aggravating) impact on the hazard (Cavallin et al. 1994; Cendrero 1997).

Once information on the severity of the sinkholes and a rough estimate of their probability of occurrence are obtained for an area, the annual potential sinkhole risk may be estimated by applying the aforementioned formula. These data may be also used to perform a cost-benefit analysis that allows us to elucidate several practical aspects for the management of the hazard (Cooper and Calow 1998; Gutiérrez 2004): (1) whether a

particular mitigation measure is cost-effective or not for a certain time period; (2) what is the time span required for a mitigation measure to break even; and (3) what are the economically or socially advantageous mitigation measures for the life time of a project.

Spain is probably the European country where subsidence caused by karstification of evaporites has the greater economic impact, and the Ebro River valley on the outskirts of the city of Zaragoza the area in Spain where sinkhole activity causes the greater amount of damage (Gutiérrez et al. 2001, 2004b; Gutiérrez 2004). Here, the generation of sinkholes is due to the karstification of Tertiary evaporites overlain by alluvial deposits, highly variable in thickness, related to the late Neogene-Quaternary evolution of the Ebro River and its tributaries (Benito et al. 1995; Soriano and Simón 1995; Gutiérrez and Gutiérrez 1998; Guerrero et al. 2004; Gutiérrez-Santolalla et al. 2005a, b). Most of the sinkhole activity (hazard) occurs in the lower alluvial levels (floodplains, younger terraces, and active and recent alluvial fans), coinciding with the areas where urban settlements, infrastructure, and human activity (exposure) tend to concentrate. Fortunately, the sinkhole hazard in the city of Zaragoza, with around 700,000 inhabitants, is low due to the large thickness of alluvium deposited in dissolution-induced basins generated by synsedimentary subsidence (Guerrero et al. 2004). However, the sinkhole activity is high in some sectors of the Ebro Valley located immediately upstream and downstream of Zaragoza. The sinkhole risk might increase substantially in the near future as this rapidly growing city expands onto some of these hazardous peripheral areas. Therefore, it is important to obtain sound quantitative information on the sinkhole hazard in these areas.

This work shows an example of a quantitative sinkhole hazard assessment in an alluvial evaporite karst area located in the periphery of the city of Zaragoza, which could be designated for the development of a new suburb of the city. Some of the methodologies that may be used to gather information with predictive utility about the spatial distribution, chronology, size, activity, subsidence mechanisms, and historical and geological evolution of the sinkholes are presented.

2 Study area: geology and geomorphology

The studied sector, 0.81 km^2 in area, is located next to the southeastern limit of the city of Zaragoza, in the southern margin of the Ebro River valley (NE Spain) (Fig. 1). It has an approximately semicircular shape in plan view and its limits are defined by the high-speed Zaragoza-Barcelona railway, the third and the fourth ring roads and a road that links both ring roads (Fig. 1). Most of the area is occupied by crop fields irrigated by sheet flooding from a dense network of irrigation ditches.

From the geological point of view, the study area is located in the central sector of the Ebro Tertiary basin, the southern foreland basin of the Pyrenees. The bedrock is made up of a thick Oligocene-Miocene evaporite sequence of the Zaragoza gypsum formation (Quirantes 1978). According to some boreholes drilled in the vicinity of Zaragoza, this formation is composed of Ca sulphates (gypsum and anhydrite), halite (NaCl), glauberite ($Na_2Ca[SO_4]_2$), marls partings and some shale units (Torrescusa and Klimowitz 1990; Ortí and Salvany 1997) in the subsurface. The presence of halite and glauberite at some depth has a special relevance since their solubilities, 360 and 118 gr/l, respectively, are much greater than that of gypsum (2.4 gr/l). In outcrop the Zaragoza gypsum formation is primarily made up of secondary gypsum after anhydrite and the incongruent dissolution of glauberite, marl partings, and shale units, indicating that the halite and glauberite beds are dissolved by underground flows as they get near the surface. These sediments show a

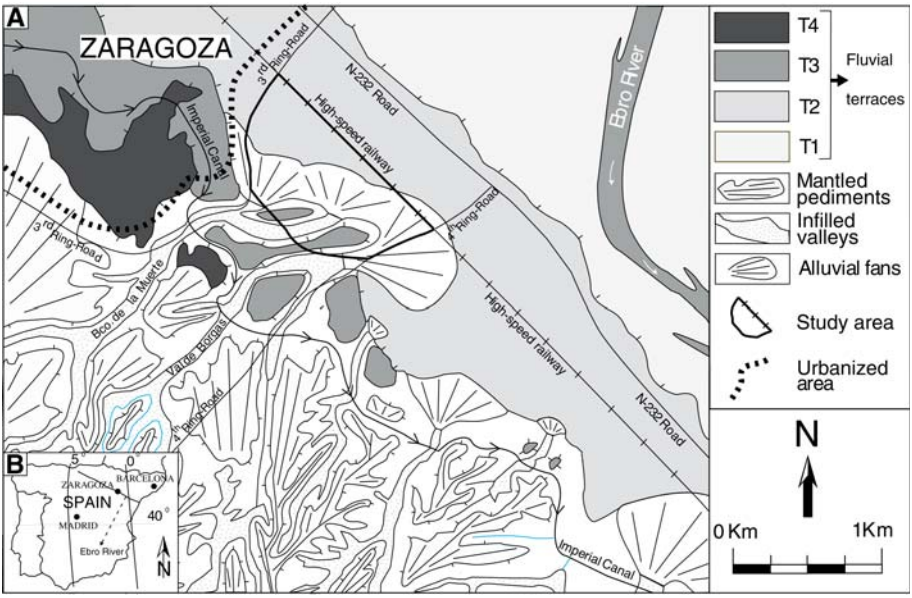

Fig. 1 Location and geomorphology of the study area

general subhorizontal structure, although they are locally affected by conspicuous gravitational deformations generated by subsidence phenomena caused by interstratal karstification (Guerrero et al. 2004). These deformations are particularly abundant in the areas where the evaporites are covered by Late Neogene-Quaternary alluvial deposits. The evaporitic bedrock is also affected by small-throw normal faults and subvertical joints with N–S, E–W and NW–SE prevalent orientations (Arlegui 1996). The NW–SE joint set, parallel to the Ebro River valley, has a marked influence on the morphogenesis (sinkholes, valley margin escarpment, and drainage network) (Gutiérrez et al. 1993, 2005a, b).

The numerous subsidence structures (paleosinkholes) exposed in natural and artificial outcrops in the area allow us to differentiate four main genetic types of sinkholes, although in many cases they show a combination of them. (1) Progressive dissolutional lowering of the rockhead with the consequent slow passive bending of the alluvial cover. The resulting subsidence sinkholes are shallow and diffuse-edged. (2) Generation of cavities (pipes, cutters) at the top of the bedrock by the enlargement of fractures and the downward migration of the overlying alluvial cover. Several deformational and transport processes may take part in the subsidence and downward migration like: ductile downward flexure, cohesive flows, granular cohesionless flows, debris-laden water flows, falls, and brittle collapse. These sinkholes are commonly cylindrical or conical in shape, generally less than 10 m in diameter, and have a considerable depth. (3) Stratigraphically controlled interstratal sheet dissolution with consequent ductile and/or brittle subsidence of the overlying bedrock and alluvial mantle. These sinkholes have a surface expression like the sinkholes of the first type, although they may reach a much larger diameter, including alluvium-filled dissolution-induced basins several kilometres across. (4) Generation of dissolutional cavities within the bedrock and upward propagation of breakdown voids by stoping processes with the formation of transtratal collapse breccia pipes. These sinkholes are morphologically equivalent to the second type, although they may reach larger

diameters. It is worth indicating that the generation of sinkholes of the first and third types (rockhead lowering and interstratal sheet dissolution) does not require the formation of cavities since the sediments overlying the dissolution horizon may settle concurrently with the evacuation of the evaporites by the groundwater. The severity of these sinkholes, formed by gradual subsidence, is much lower than the severity of the other two types, which may occur in a catastrophic way without any noticeable previous warning. On the other hand, the volume at the time of formation of the sinkholes of the second and fourth types provides a minimum estimate of the volume of the collapsed subsurface voids. The volume of old sinkholes that may have undergone reactivations only provides a minimum estimate of the volume of the dissolved soluble rocks. Unfilled voids may still exist in the subsurface and the brittle deformation of the sediments overlying dissolution cavities or horizons may lead to a substantial decrease in density.

The interpretation of aerial photographs and field surveys allowed us to differentiate four morphosedimentary units in the study area (Fig. 2):

- Upper terrace: this Ebro River terrace is located in the southern sector of the area. Here the terrace surface lies 26 m above the Ebro River channel. A borehole drilled on this surface (borehole 1, Fig. 2) crossed 42 m of alluvium, indicating that subsidence phenomena caused by the karstification of the bedrock operated in this sector concurrently with the deposition of the terrace. The best exposure found in an old

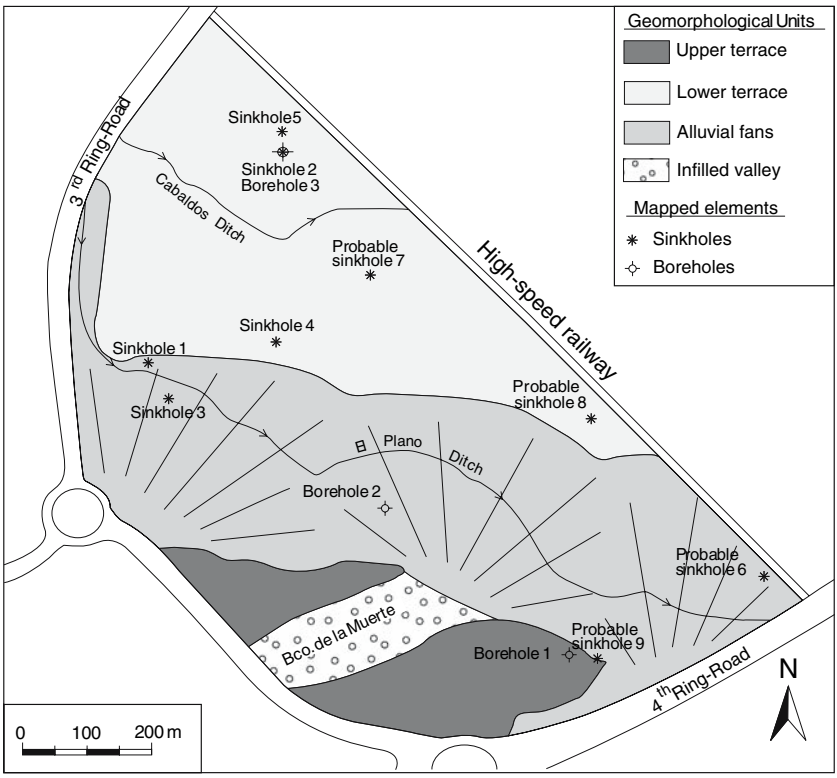

Fig. 2 Geomorphological map of the study are indicating the location of the sinkholes, probable sinkholes, and boreholes

gravel pit showed 2.5 m of fluvial gravels overlaid by 1 m of alluvial fan deposits made up of silts and sands with scattered pebble and cobble gravels. In the eastern sector of the aggregate pit, the fluvial gravel unit is locally tilted and crossed by a 50-cm-wide vertical conduit filled with silts and clasts that show reoriented vertical fabrics next to the margins (Fig. 3). The pipe, truncated and fossilized by the undeformed alluvial fan unit, has been interpreted as a collapse chimney, formed before the accumulation of the fan deposit by downward migration of the fluvial deposits towards karstic conduits developed in the evaporitic substratum.

- Lower terrace: the surface of this terrace, located in the northern sector of the area, lies 10–15 m above the Ebro River channel. The deposits underlying the terrace flight are composed of a variable proportion of channel gravel and overbank fine-grained facies. Its thickness reaches 31 m in borehole 3, drilled in an active sinkhole (sinkhole 2), and 26 m in borehole 2 (Fig. 2). The anomalously high thickness is indicative of synsedimentary karstic subsidence. It is possible that the alluvium sequence beneath this terrace tread may correspond to the stacking of the sedimentary units of two or more terraces (Gutiérrez 1996; Benito et al. 1998).
- Flat-bottom infilled valleys: this unit corresponds to a small infilled valley excavated in the upper terrace (Fig. 2). This currently inactive valley is one of the main channels of the Barranco de la Muerte, which shows a bifurcation close to its mouth (Fig. 1). The valley is filled by several meters of gypsiferous silts with scattered clasts and gravel layers.

Fig. 3 Alluvium-filled pipe in the deposit of the upper terrace truncated and overlaid unconformably by an undeformed alluvial fan unit. Note the reoriented subvertical fabrics of the clasts in the pipe fill

- Alluvial fans: between the two terraces, the topography and the underlying deposits allowed us to identify three coalescing alluvial fans feed by the Barranco de la Muerte (the two western ones) and the Val de Borgas (the eastern one) (Figs. 1, 2). The alluvial fan deposits overlap the fluvial sediments of the lower terrace and are made up of tabular silt layers with some clasts up to 20 cm long (sheet flood deposits).

3 Analysis of the sinkholes

The identification and analysis of the sinkholes was carried out in two phases. The initial phase focused on the identification of sinkholes and features attributable to sinkholes based on a thorough field survey and analysis of all available sources of information. The work done in the second phase aimed at elucidating whether questionable features corresponded to actual sinkholes and analysis of the underground structure, geochronology, and evolution (subsidence mechanisms and rates) of a particular sinkhole (trenching and drilling).

3.1 Initial identification phase

In addition to the detailed field surveys, the following sources of information were investigated to obtain an exhaustive database of sinkholes from the study area: (1) interviews with the local residents, (2) records from consulting companies, (3) newspaper reports, (4) previous geomorphological maps, and (5) old topographical maps (these documents may help to pinpoint buried dolines from the mapped features or the local names), (6) detailed topographical maps, and (7) aerial photographs. The old topographical maps studied include documents from 1852, 1866, and 1892 with scales ranging from 1:10,000 to 1:50,000. No information on sinkholes could be derived from these maps in this case. Two detailed topographical maps with contour line intervals of 1 m were examined with successful results:

- A topography 1:2,000 in scale produced in 1935 for the Zaragoza Council.
- The so-called Galtier topography of the Zaragoza Council, elaborated in 1971–1974 at a scale of 1:1,000.

The aerial photographs studied included orthophotos from 1927 and 1998 with scales of 1:10,000 and 1:5,000, respectively, and aerial photographs for stereoscopic interpretation from August 1956 (1:30,000), October 1984 (1:30,000), June 1986 (1:18,000), and May 2004 (1:3,500).

Five sinkholes and four locations with features that could be attributable to karstic subsidence (probable sinkholes) were identified in this initial identification phase (Fig. 2 and Table 1).

3.1.1 Sinkhole 1

This buried sinkhole, located on the western fan next to the El Plano Ditch (Fig. 2), was recorded thanks to information supplied by several local residents who indicated that the collapse doline formed five or six decades ago and was filled in the beginning of the 1990s. The sinkhole can be recognized in the 1927 orthophoto as a circular area devoid of

Table 1 Type, morphometry, distance to the nearest neighbour (*L*) and chronology of the sinkholes

Sinkhole	Type	Diameter (m)	Depth (m)	Area (m^2)	Volume (m^3)	*L* (m)	Date of formation (years)
1	Collapse	12–14	4	113–154	452–616	63	pre-1927
2	Collapse/bending	16	0.4	201	80	30	pre-1971–74
3	Collapse	5	18–20	20	700	63	16 February 2002
4	Collapse	11–12/5	2.5/4	95–113/20	238–283/80	180	pre-1927/12 May 2002
5	Collapse	2	?	3	?	30	?
6?	*?*	*4*	*0.5?*	*13*	*6?*	*258*	*pre-1984*
7?	*?*	*1*	*0.5*	*1*	*0.5*	*180*	*?*
8?	*?*	*6*	*0.2*	*28*	*7*	*355*	*?*
9?	*?*	*1 × 0.5*	*>4*	*0.5*	*>2*	*258*	*?*
Total 1				533.5	1694.5		
Total 2				491	1679		

Note: Total 1 refers to the values obtained in the first phase of the study considering the identified and probable sinkholes. Total 2 correspond to the final figures calculated after ruling out the four probable sinkholes (in italics) by trenching

vegetation and in the 1956 aerial photographs as a topographic depression (Fig. 4). The doline is clearly depicted in the Galtier topography from 1971–1974 as a depression 12–14 m in diameter and 4 m deep located 5 m to the north of the El Plano Ditch (Fig. 4). Very probably, the sinkhole was formed before 1927 and filled between 1971–74 and 1984, although it is not present in the 1935 topography. Consequently, the sinkhole is more than 78 years old and the infill took place between 34 and 20 years ago. Inspection of the area and the information provided by the local residents suggest that this sinkhole has not undergone recent reactivations. The excavation of four trenches allowed us to locate the sinkhole more precisely.

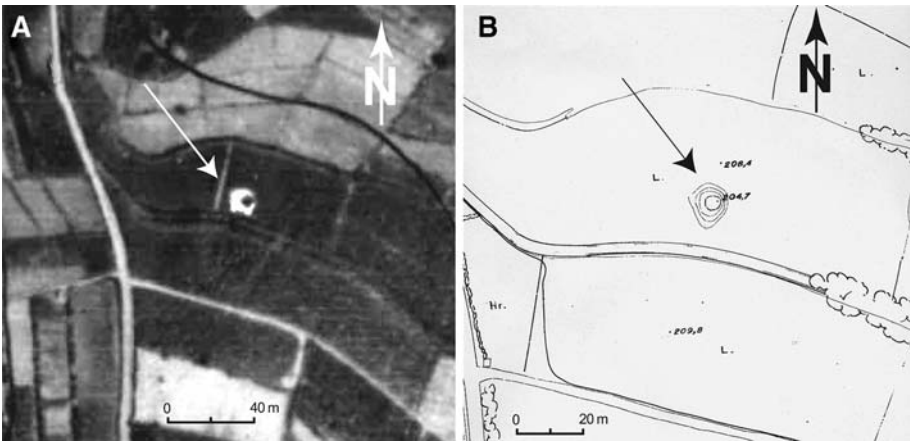

Fig. 4 (**A**) Sinkhole 1 in the 1927 orthophoto; (**B**) sinkhole 1 in the 1971–1974 topography of the Zaragoza Council (1:1,000 in scale, contour interval 1 m)

Fig. 5 Image of sinkhole 2 (December 2004). Note the higher density of grass vegetation and the reeds growing in the crop field boundary. The city of Zaragoza can be seen in the background

3.1.2 Sinkhole 2

This diffuse-edged sinkhole, 16 m in diameter and 0.4 m deep, is located in the northern sector of the lower terrace (Fig. 2) and affects two contiguous crop fields (Fig. 5). The margin of the sinkhole shows discontinuous tension cracks and aligned pipes, probably generated by the collapse of cavities produced by the downward migration of alluvium through open cracks. The bottom of the sinkhole has a higher density of grass vegetation than the surrounding area and the gravels dumped on the boundary between the crop fields to raise the topographic surface are colonized by reeds (*Pragmites* sp.). This sinkhole is reflected in the elevation data of the 1971–1974 topography and is recognizable in the aerial photographs taken in 1984, 1986, 1998, 2000, and 2004. From these data we can infer that the sinkhole formed before 1971–1974. Probably it was older than 1927 and it has not been detected in the 1927 and 1956 images due to the impossibility of getting stereoscopic view from the former and the reduced scale of the latter. The conspicuous geomorphic expression of the sinkhole in crop fields under exploitation, the evidence of instability (cracks and pipes), and the recent anthropogenic fill reveal that it corresponds to an active sinkhole. However, the strongly disturbed morphology of the sinkhole does not allow us to delineate its limits precisely and to infer the subsidence mechanisms and rates.

3.1.3 Sinkhole 3

This sinkhole, whose occurrence on 16 February 2002 was widely covered by the local media, formed in the western fan 30 m south of El Plano Ditch (Figs. 2, 6A and B). The flood caused by the failure of the Imperial Canal a few days before might have triggered the opening of the collapse sinkhole, which was 18–20 m deep and 5 and 8–10 m across at the ground surface and at the bottom, respectively. This is the deepest sinkhole documented in the Ebro Valley according to the information gathered by the authors. No evidence of previous activity has been detected at this location in the detailed topographical maps and in the aerial photographs. The hollow was filled soon after its formation with a wide variety of poorly sorted waste material (gravels, rubble material, concrete blocks, etc.). A sinkhole 5 m in diameter and 3 m deep was observed in a survey carried in December 2004 (Fig. 6C). Very probably this settlement was due to the

Fig. 6 (**A**) Sinkhole 3 formed on 16 February 2002; (**B**) close-up view of sinkhole 3. Photographs **A** and **B** were taken a few days after the formation of the collapse doline; (**C**) sinkhole 3 on December 3, 2004. This depression was very likely due to the compaction of the anthropogenic fill

compaction of the fill and the downward migration of fine particles through the void spaces. The sinkhole is not shown in the images taken in May 2004, indicating that reactivation took place that year between May and December. The sinkhole was buried again as it did not show any surface expression in November 2005. The dimensions of the sinkhole formed in February 2002 indicate that its generation is related to a cavity developed in the evaporitic bedrock with a volume of more than 700 m^3. The dissolution cavity gave place to a collapse cavity by the breakdown and downward migration of the ceiling material (ravelling and stoping). The void propagated upward and eventually intercepted the ground surface, generating the collapse sinkhole.

3.1.4 Sinkhole 4

This collapse sinkhole, around 5 m across and 4 m deep, opened on May 12, 2002 undermining a small storehouse located next to the distal limit of the western fan (Figs. 3, 7A and B). The hollow was filled soon after its occurrence. According to local residents, in this location there used to be a sinkhole 11–12 m in diameter and around 2.5 m deep whose circular bottom was used as a market garden. The depression was filled with aggregates and the storehouse was partially built on the infilled sinkhole. This information indicates that the collapse sinkhole that occurred in 2002 corresponds to a reactivation of a previously existing doline. The old sinkhole can be recognized in the aerial photographs taken in 1927 and 1956. The storehouse can be identified in the 1984 images but not the old sinkhole, indicating that the previous doline formed more than 78 years ago and was filled between 1956 and 1984. In the survey conducted in December 2004 the only evidence of

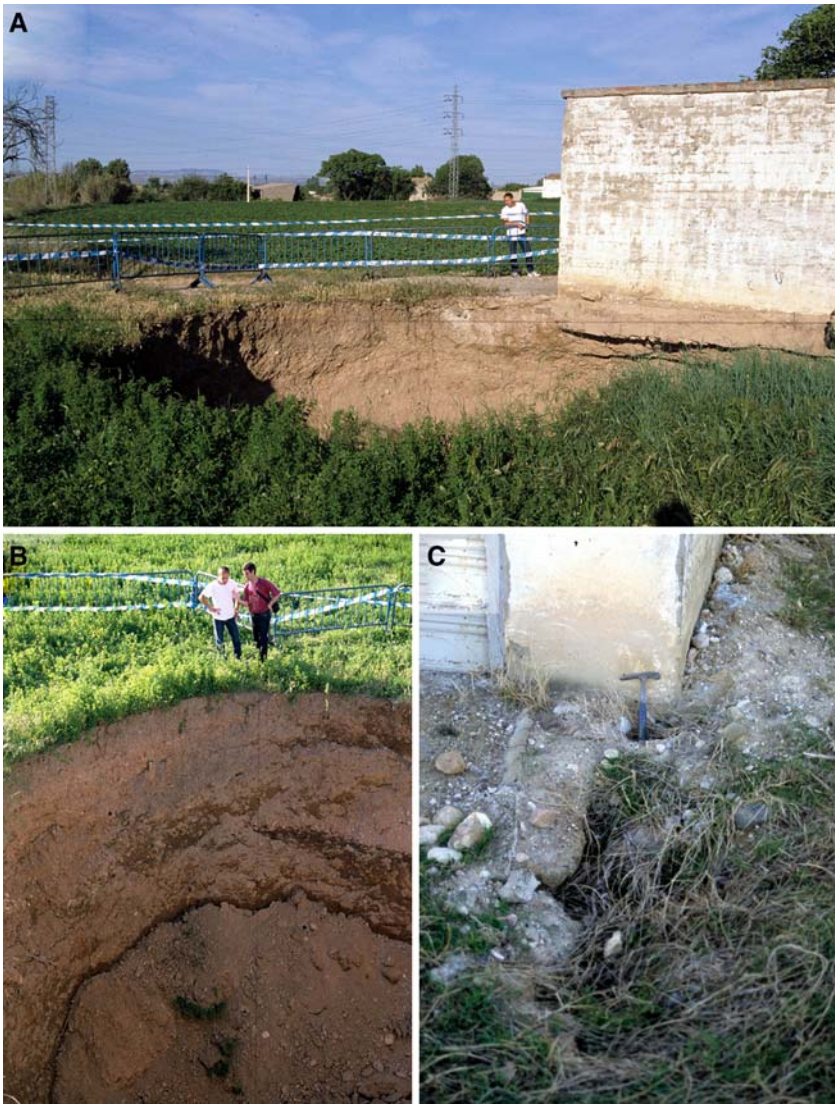

Fig. 7 (**A**) Sinkhole 4 formed on May 12, 2002; (**B**) close-up view of sinkhole 4. Photographs **A** and **B** were taken on 14 May 2002; (**C**) crack affecting the sinkhole fill in December 2004

instability corresponded to a crack 80 cm long open in the fill material located next to the northwestern corner of the building (Fig. 7C).

3.1.5 Sinkhole 5

This sinkhole is located in a crop field on the lower terrace, very close to sinkhole 2 (Fig. 2). Its location was reported by the farmer who cultivates the crop field. According to

this farmer, it corresponds to a depression 2 m diameter that needs to be frequently filled. The low number of blows (<10) recorded in a penetration test 14.6 m deep performed at this location suggests that it may correspond to an active collapse chimney.

3.1.6 Probable sinkhole 6

This probable sinkhole corresponds to an elongated depression 4 m long and filled with blocks located at the margin of a crop field adjacent to the fourth ring road (Fig. 2). Several decimetric pipes have been observed in the surroundings of the depression. The 1984 and 2000 aerial photographs show a decrease in the vegetation density in this location. It is not clear whether this feature corresponds to a filled subsidence feature or not.

3.1.7 Probable sinkhole 7

This depression has been found on the lower terrace next to an unlined ditch (Fig. 2). It is a circular and scarp-edged hollow 1 m in diameter and 0.5 m deep filled with large blocks. It is not clear whether this feature corresponds to a scour generated by irrigation waters derived from the adjacent ditch or a small collapse sinkhole.

3.1.8 Probable sinkhole 8

This feature, located on the lower terrace, corresponds to a very shallow depression 6 m in diameter with an anomalously high concentration of reeds (*Pragmites* sp.) (Fig. 2). These features could be indicative of active subsidence.

3.1.9 Probable sinkhole 9

A slightly inclined hollow 1 m in diameter has been detected at the foot of the upper terrace scarp and next to a gravel pit (Fig. 2). It is not clear if this feature corresponds to an artificial excavation or an old sinkhole.

3.1.10 Preliminary hazard assessment

Previous studies carried out in various sector of the Ebro Valley provide some rough estimates of the density of sinkholes, the percentage of the area covered by sinkholes or the probability of the occurrence of sinkholes:

- In a sector of the low terrace of the Ebro River located in the southern flank of the valley upstream of Zaragoza, Soriano (1990) estimated a density of 22 sinkholes/km^2. In a particular zone of this terrace, 21 km^2 in area, van Zuidam (1976) used aerial photographs of different dates to identify 35 new sinkholes formed during a time span of 18 years. These values yield a minimum estimate of 0.09 sinkholes/km^2 year for the probability of occurrence of sinkholes. The actual figure may be much larger since a significant number of the sinkholes formed during the considered time span may have

not been identified due to the small scale of the aerial photographs used by the author (1:30,000–40,000) and/or their anthropogenic infill.

- In the northern margin of the Ebro River valley, downstream of Zaragoza and close to the village of La Puebla de Alfindén, there is a particularly active sinkhole field (0.25 km^2) developed on alluvial fans. Here, Gutiérrez-Santolalla et al. (2005b) mapped 158 collapse sinkholes and estimated a sinkhole density higher than 600 sinkholes/km^2, a percentage area covered by sinkholes of around 20%, and a probability of occurrence of sinkholes of several sinkholes/km^2 year.
- In the stretch of the Ebro River floodplain between Zaragoza and El Burgo de Ebro the mapped subsidence sinkholes cover more than 10% of the area (Gutiérrez-Santolalla et al. 2005a). Recent detailed studies conducted in a profusely irrigated terrace in the El Burgo de Ebro area indicate a minimum probability of occurrence of 40 collapse sinkholes/km^2 year. The sinkholes that occur in this area are induced to a great extent by irrigation (sheet flooding) and are commonly 1–1.5 m in diameter (Gutiérrez et al. 2006).

In our study area, the available information at this initial investigation phase on verified sinkholes (five) and probable sinkholes (four) allows us to obtain estimates for the sinkhole density and the percentage of sinkhole area of 11.1 sinkholes/km^2 and 0.066%, respectively (Table 1). These values may be considered as conservative approximations, since we may expect that most of the recent sinkholes with or without surface expression have been identified and that some of the features regarded as probable sinkholes may not correspond to karstic depressions. In spite of this, the calculated sinkhole density and percentage of sinkhole area are lower than the values obtained for other sectors of the Ebro Valley in the outskirts of Zaragoza (Soriano 1990; Gutiérrez-Santolalla et al. 2005a, b). The low percentage of sinkhole area clearly reflects the small size of the sinkholes of the study area in comparison with the sinkholes that occur in other nearby zones (floodplain and low terraces upstream of Zaragoza).

The absolute and relative chronological data on the formation of sinkholes allows us to calculate a preliminary probability of the occurrence of sinkholes of 0.14 sinkholes/km^2 year (9 sinkholes/0.81 $km^2 \times 78$ years) and an annual probability of sinkhole occurrence of 11.34% ($0.14 \times 100 \times 0.81$) (Table 2). These values may be considered as conservative

Table 2 Morphometric parameters and values related to the spatial distribution and probability of occurrence of sinkholes

Area of the study zone (km^2)	0.81	
Number of sinkholes	9	5
Sinkhole density (D) number of sinkholes/km^2	11.1	6.17
Total sinkhole area (km^2)	0.000533	0.000491
Percentage of sinkhole area (%)	0.066	0.060
Probability of occurrence of sinkholes (sinkholes/km^2 year)	0.14	0.079
Annual probability of occurrence of sinkholes (%)	11.34	6.41
Mean distance to the nearest neighbour (L_a) km	0.157	0.075
Theoretical mean distance to the nearest neighbour ($L_e = 1/2\sqrt{D}$) km	1.66	1.24
Spatial distribution index ($R = L_a/L_e$)	0.09	0.06

Note: The first column corresponds to the figures obtained in the first investigation phase (sinkholes and probable sinkholes) and the second column to the more-realistic calculations of the final investigation phase after ruling out the four probable sinkholes by trenching

estimates since some of the sinkholes were formed more than 78 years ago and some of the probable sinkholes may not correspond to actual sinkholes. A more-precise probability evaluation could be achieved by checking whether the features considered as probable sinkholes actually correspond to sinkholes or not.

3.2 Final checking and analysis by trenching

In a second investigation phase, a trenching program, accompanied in a particular case by a detailed study of the stratigraphy and structure of the exposed deposits and the application of absolute dating methods, was conducted in order to elucidate the nature of the probable sinkholes and obtain additional information on sinkhole 2. This investigation technique, commonly used in paleoseismological (e.g., McCalpin 1996) and landslide (e.g., Gutiérrez-Santolalla et al. 2005c) investigations, is proposed as a useful and cost-effective methodology to gather practical information with predictive utility on particular sinkholes or subsidence features. It may provide insight on the precise location of filled and poorly defined sinkholes, their internal structure, the genetic mechanisms and the subsidence history, including the differentiation of subsidence episodes, their magnitude and the chronology (relative or absolute) and rate of the subsidence, either continuous or episodic.

The 1.8–4.5-m-deep backhoe trenches dug in each of the probable sinkholes 6–9 (Fig. 2) showed the lack of deep fill materials and deformational structures, allowing us to rule out a karstic origin. In all these cases the exposed deposits showed a clear horizontal structure with no evidence of postdepositional disturbance. Consequently, these probable sinkholes considered in the preliminary hazard analysis could be safely discarded, restricting the number of sinkholes for a subsequent hazard analysis.

Sinkhole 2 was investigated by digging three backhoe trenches aligned in the N40E direction (Figs. 8, 9) and drilling a 31-m-deep rotary percussion borehole (borehole 3) in the central and lower point of the depression (Fig. 2). The longest trench (trench 1), which was 13 m long and 4.3 m deep, had its SW end located in the centre of the sinkhole. The other two trenches (trenches 1 and 2), which were 3 and 2.8 m deep, respectively, were dug outside the sinkhole and to the NE of trench 1 (Fig. 9). The following units were differentiated in the drillhole from the top to the base: (1) 8.5 m of anthropogenic fill made up of dark clays with scattered clasts including brick and slag fragments; (2) 4 m of dark orange overbank fines (Tf); (3) 6 m of gravels with a sandy-silty matrix (Tg); (4) 12 m of strongly weathered bedrock composed of grey and dark green marls with gypsum fragments and small voids near the base (Rk); (5) unweathered gypsiferous bedrock at 31 m (Bg).

The information supplied by the trenches and borehole indicate that in this location the terrace deposit is composed of a lower gravel unit 6 m thick (Tg) and an upper overbank fines unit made up of dark orange silts (Tf), whose thickness varies from 2.3 m in trench 3 to 4 m in the NE tip of trench 1 (Fig. 8). Assuming that the top of the gravel unit (Tg) was an approximately horizontal surface at the time of its deposition, the gradual thickening of the overbank fines unit (Tf) towards the centre of the sinkhole records the presence of a bending paleosinkhole larger than the current sinkhole that was active concurrently with the deposition of the upper terrace unit (Tf) and probably also during the deposition of the lower gravel unit (Tg). The magnitude of this synsedimentary subsidence reached at least 1.7 m, the thickness variation of Tf between trenches 1 and 3 (Fig. 8).

Three samples of carbonaceous material for radiocarbon dating were collected from the unit of overbank fines in trench 1 at depths of 110, 180, and 280 cm (B-110, B-180, and B-280) (Fig. 9B). Unfortunately the results obtained from the Beta Analytic Laboratory

Fig. 8 Trench 1 dug in sinkhole 2

were not consistent with the local stratigraphy and chronology of the fluvial terraces. The amount of carbon in the B-110 sample was insufficient even for the application of the accelerator mass spectrometry (AMS) technique. The B-180 sample yielded a calibrated age of 1,410 years BP and the age of the B-280 sample was older than the range of the applied geochronological method (>47,600 years BP). According to the available chronology of the fluvial terraces in the Ebro Basin (Andres et al. 2002; Sancho et al. 2004), the age obtained from the B-280 sample (>47,600 years BP) is much older than the expected age for the lower terrace located 10–15 m above Ebro River channel. The scant sampled material may correspond to reworked older detrital particles. On the other hand, the calibrated age of the B-180 sample (1,410 cal years BP or 540 years AD) is excessively young for this terrace considering that, according to the archaeological studies of the Roman city of Caesaraugusta, the Ebro River was at that time at an elevation similar to that of the present time (Aguarod and Erice 2003). The available information allows us to infer that, during the deposition of the terrace, at this location there was an active sinkhole probably more than 80 m in diameter affected by gradual passive bending. The magnitude of the subsidence that operated during the deposition of the upper overbank fines terrace unit was higher than 1.7 m. Regretfully, the inconsistency of the radiocarbon dates obtained does not permit the determination of the timing of this subsidence period or the subsidence rate. The flexure that generated this sinkhole could be due to the progressive

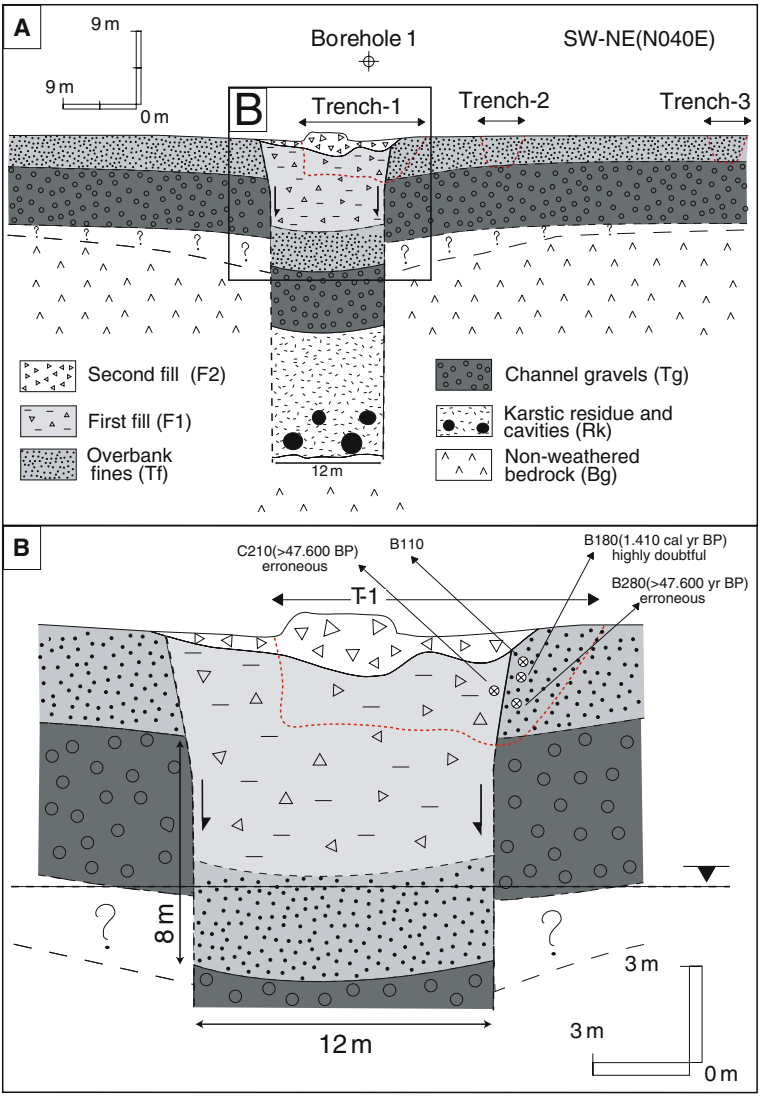

Fig. 9 Cross sections of sinkhole 2 based on borehole 1 and the interpretation of trenches 1, 2, and 3. The position of the collected samples for radiocarbon dating and the obtained ages are indicated

differential lowering of the rockhead, a stratigraphically controlled interstratal karstification, or a combination of both (Fig. 10).

Trench 1 exposed a well-defined subvertical plane that juxtaposed the gravels and fines of the terrace against an anthropogenic fill (F1) made up of a massive dark argillaceous deposit with floating clasts including fragments of pottery and brick and abundant carbonaceous fragments (Fig. 9B). This plane could correspond to a collapse failure plane (gravitational fault) affecting the fill F1, or the abrupt margin of a collapse sinkhole (scarp) previous to the fill F1. The latter option seems to be more likely since the plane is locally

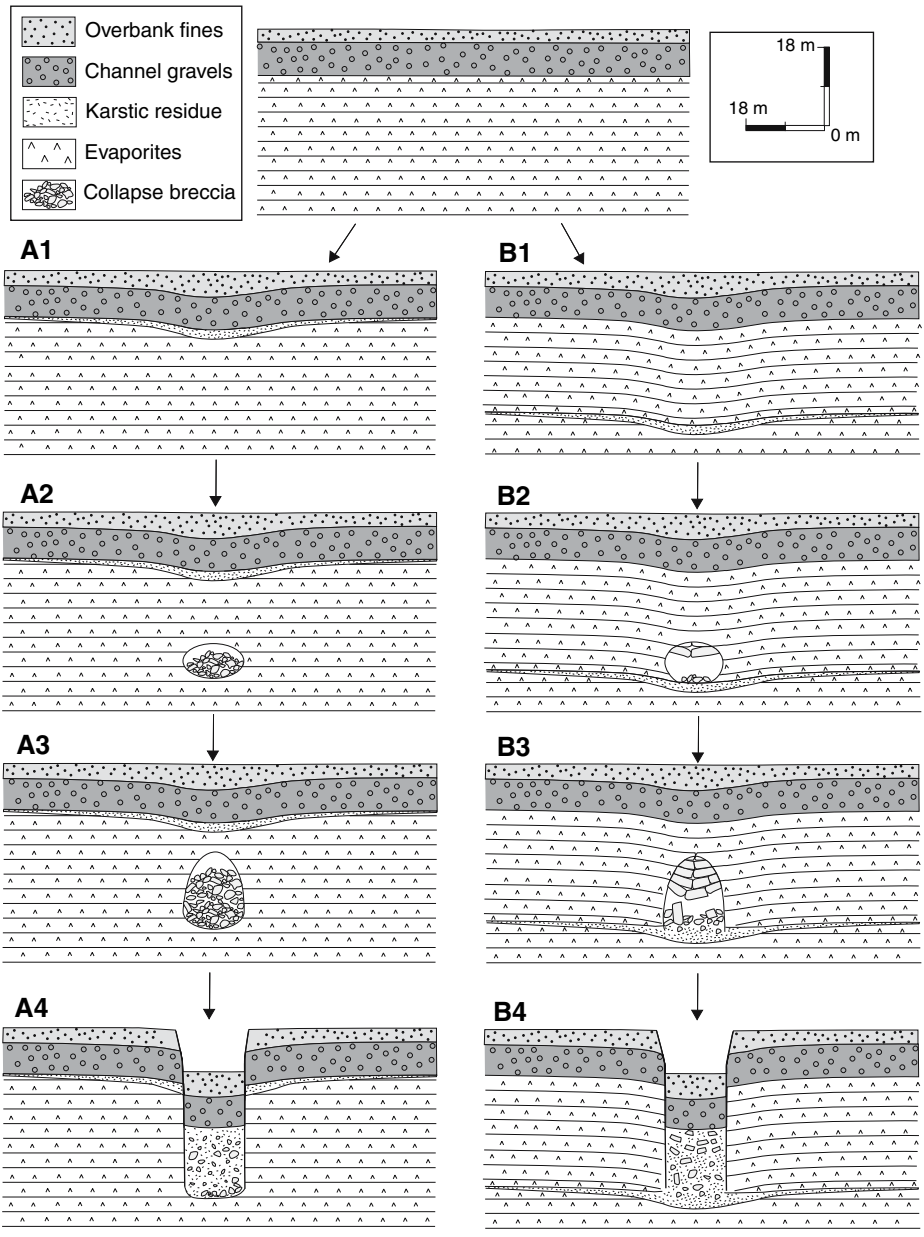

Fig. 10 Two possible evolutionary histories of sinkhole 2. The sinkhole generated by synsedimentary bending is due to dissolution at the rockhead in option A and to interstratal karstification in option B

irregular and no evidence of relative movement and friction between the two adjoining materials (reoriented clasts, shear bands) was observed. The sample collected from this fill at a depth of 210 m (C-210) has yielded an age of >47,600 years BP (Fig. 9). It is obvious that this age is not correct since this first anthropogenic fill must be historical and younger

than the adjacent terrace deposits. Unfortunately, this indicates that the sampled material was inappropriate (potentially reworked material or slag fragments).

Both the anthropogenic fill F1 and its bounding subvertical plane are overlapped by a second undeformed fill (F2). This deposit, composed of gravels with a sandy matrix including very recent man-made objects (ornamented pottery, wires, plastic bags, a shoe sole), fills a depression with an undulated topography (Fig. 9). The content of this second fill indicates an age younger than 50 years.

The subvertical plane that bounds the older fill (F1) and the terrace deposit indicates that the analyzed sinkhole has undergone collapse subsidence in historical times. The vertical structural throw of the top of the gravel unit indicates a subsidence magnitude of 8 m in this collapse sinkhole superimposed on an inactive larger subsidence sinkhole. Probably the vertical offset records a cumulative displacement resulting from multiple collapse events. Regarding the chronology of the collapse, although it could have been active during the deposition of the terrace concomitantly with the development of the larger subsidence sinkhole, postsedimentary collapse is considered the most likely option. In this case the initiation of the collapse sinkhole would be subsequent to the age of the top of the terrace deposit and previous to the older fill (F1). The age of the fill F1 would predate the last collapse event if the bounding plane corresponds to a failure plane and it would postdate it if the plane corresponds to a buried sinkhole scarp. Assuming revolution symmetry for the collapse structure with its centre coinciding with the lowest point of sinkhole 2, a diameter of 12 m and an approximate volume of 900 m^3 can be estimated. Very probably this sinkhole resulted from the progressive upward stoping of a cavity more than 900 m^3 in volume developed at some depth within the evaporitic bedrock. Superimposed subsidence structures similar to those illustrated in Fig. 10 have been documented from artificial exposures in the Ebro Valley (Guerrero et al. 2004).

4 Hazard assessment

The additional information gained by the trenching program in the second investigation phase allows us to obtain more-realistic parameters related to the sinkhole hazard of the area. After ruling out the four probable sinkholes, a density of 6.17 sinkhole/km^2 and a percentage of sinkhole area of 0.060% are obtained. The new sinkhole density is 44% lower than the former one (11.1 sinkholes/km^2). The new figures indicate that the area has a number of sinkholes per unit area and percentage of sinkhole area considerably lower than other sectors of the Ebro Valley in the outskirts of Zaragoza (Soriano 1990; Gutiérrez-Santolalla et al. 2005a, b).

The minimum age of 78 years for the five sinkholes in the 0.81 km^2 area yields a probability of occurrence of 0.079 sinkholes/km^2 year and an annual probability of sinkhole occurrence of 6.4% ($0.079 \times 100 \times 0.81$). The ruling out of the probable sinkholes through the trenching program has led to a reduction of 44% of the previously estimated spatiotemporal probability. Regarding severity, information derived from the human and geological record indicates that the sinkholes that occur in the study area commonly result from the catastrophic collapse of subsurface voids and that they may reach 10–15 m in diameter at the time of formation.

Several aspects related to the spatial distribution of the sinkholes may be used to derive some considerations about relative sinkhole spatial susceptibility in the area:

- The concentration of all the identified sinkholes in the northwestern sector of the area (lower terrace and western fan) indicates a higher likelihood of new sinkhole occurrences for this portion.
- No sinkholes have been identified in the upper terrace within the limits of the study area or beyond. This is probably due to the fact that the deposits of this terrace are more indurated than those of the lower terrace.
- It seems that the areas located close to the irrigation ditches are more prone to the formation of new sinkholes.
- The five verified sinkholes yield a spatial distribution index (R) of 0.06. This index quantifies the clustering or dispersion of the sinkholes (Clark and Evans 1954; Williams 1972). $R = 1$ indicates a random distribution, $R = 0$ a maximum clustering, and $R = 2.1491$ the maximum dispersion with a uniform hexagonal pattern. The calculated index shows that the sinkholes of the study area tend to form clusters, suggesting that the vicinity of the existing sinkholes has a relative higher susceptibility.

Based on the previously indicated considerations the following relative susceptibility zonation can be proposed from higher to lower probability: (1) the periphery of the existing sinkholes, (2) the northwestern sector and areas close to ditches, (3) the remaining area except the upper terrace, and (4) the upper terrace.

5 Conclusions

The main conclusions derived from this work include:

- The quantitative assessment of the sinkhole hazard in karst areas is a crucial task for the effective management of the frequently underestimated sinkhole risk. The hazard assessments should address two aspects: the probability of occurrence of sinkholes (sinkholes/km^2 year) and the severity of the sinkholes, which mainly refers to the subsidence mechanisms (gradual subsidence or catastrophic collapse) and the size of the sinkholes at the time of formation.
- Hazard assessments should be based on an exhaustive database of recent sinkholes, including information on the location and chronology of the sinkholes (probability of occurrence), and the size of the sinkholes at the time of formation and their subsidence mechanisms and rates (severity). In most cases the hazard assessments are minimum or optimistic predictions, since it is difficult to obtain records for all the sinkholes formed in the time span considered. Some of the sources of information that may be investigated for the elaboration of the sinkhole database include: thorough field surveys, accounts from local residents and farmers, newspaper reports, records from consulting companies and governmental agencies, historical and modern topographical maps, geomorphological maps, aerial photographs from different dates, and site geotechnical investigations (e.g., trenching, boreholes, and geophysics).
- The hazard assessment conducted in the alluvial evaporite karst study area has allowed us to estimate a probability of occurrence of 0.079 sinkholes/km^2 year (6.4% annual probability) and to foresee catastrophic collapse sinkholes that may reach 10–15 m in diameter.
- The trenching program carried out in a final site investigation phase allowed us to rule out four doubtful sinkholes, reducing by 44% the preliminary estimation of the probability of occurrence of sinkholes.

- The evolutionary history of one of the sinkholes has been inferred through detailed study of the deposits and deformational structures exposed by trenching. This has led to the identification of a historical collapse sinkhole around 12 m across with a cumulative subsidence of 8 m, superimposed on a subsidence sinkhole approximately 80 m across that records a synsedimentary subsidence greater than 1.7 m. Unfortunately, the inconsistency of the obtained radiocarbon ages did not allow us to determine the chronology of the subsidence periods and the mean subsidence rates.
- Trenching accompanied by the application of dating techniques is proposed as a useful method for gathering information with predictive utility on the evolution of sinkholes in alluvial karst settings. The trench exposures may help to elucidate the genesis of doubtful features attributable to karstic subsidence, locate the precise boundaries of the subsidence structures, and establish the size of the sinkholes at the time of formation. The retrodeformation analysis of the subsidence-affected sediments permits one to differentiate subsidence episodes and infer their magnitude and mechanisms. Key geochronological information may allow us to constrain the timing of the subsidence episodes and calculate subsidence rates.

Acknowledgements The authors would like to thank José Ángel Navamuel and the Urban Development Engineering Unit of the Zaragoza Council for supporting the investigation. This work has also been cofinanced by the Spanish Education and Science Ministry and the FEDER (project CGL2004-02892/BTE). We are also grateful to Mr. Octavio Plumed from the company ENTECSA for his valuable contribution to this work.

References

Aguarod C, Erice R (2003) El Puerto de Caesaraugusta, in IV Jornadas de Arqueología subacuática. Valencia, pp 143–155

Andres W, Ries J, Seeger M (2002) Pre-holocene sediments in the Barranco de las Lenas, Central Ebro Basin, Spain, as indicators for climate-induced fluvial activities. Quatern Int 93–94:65–72

Arlegui L (1996) Diaclasas, fallas y campos de esfuerzo en el sector central de la Cuenca del Ebro. Ph.D. Thesis, University of Zaragoza, 308 p (In Spanish, unpublished)

Ayala-Carcedo FJ (2002) Introducción al análisis y gestión de riesgos. In: Ayala-Carcedo FJ, Olcina J (coords) Riesgos naturales. Ariel Ciencia, Barcelona, pp 133–145

Beck BF (1991) On calculating the risk of sinkhole collapse. In: Kastning EH, Kastning KM (eds) Appalachian karst. Proceedings of the Appalachian karst symposium. National Speleological Society, Radford, Virginia, pp 231–236

Bell FG (1999) Geological hazards. Their assessment, avoidance and mitigation. E & FN Spon, London, p 648

Benito G, Pérez del Campo P, Gutiérrez-Elorza M, Sancho C (1995) Natural and human-induced sinkholes in gypsum terrain and associated environmental problems in NE Spain. Environ Geol 25:156–164

Benito G, Gutiérrez F, Pérez-González A, Machado MJ (1998) River response to Quaternary subsidence due to evaporite solution (Gallego River, Ebro Basin, Spain). Geomorphology 22:243–263

Bezuidenhout CA, Enslin JF (1970) Surface subsidence and sinkholes in the dolomitic areas of the Far West Rand, Transvaal, Republic of South Africa, Land Subsidence. Int Assoc Hydrol Sci, Publ. 89:482–495

Cavallin A, Marchetti M, Panizza M, Soldati M (1994) The role of geomorphology in environmental impact assessment, Geomorphology 9:143–153

Cendrero A (1997) Riesgos naturales e impacto ambiental, In: Villaverde MN, Tébar RL (coords) La Interpretación de la Problemática Ambiental: Enfoques Básicos II. Fundación Universidad-Empresa, Madrid, pp 23–90

Clark PJ, Evans FC (1954) Distance to nearest neighbour as measure of spatial relationships in populations. Ecology 35:445–453

Cooper AH, Calow RC (1998) Avoiding gypsum geohazards: guidance for planning and construction. British Geological Survey Technical Report WC/98/5, 57 p

Crozier MJ, Glade T (2004) Landslide hazard and risk: issues, concepts and approach. In: Glade T, Anderson M, Crozier MJ (eds) Landslide hazard and risk. John Wiley & Sons, Chichester, pp 1–40

Guerrero J, Gutiérrez F, Lucha P (2004) Paleosubsidence and active subsidence due to evaporite dissolution in the Zaragoza city area (Huerva River valley, NE Spain). Processes, spatial distribution and protection measures for linear infrastructures. Eng Geol 72:309–329

Gutiérrez F (1996) Gypsum karstification induced subsidence (Calatatud Graben, Iberian range, Spain). Geomorphology 16:277–293

Gutiérrez F (2004) El riesgo de dolinas de subsidencia en terrenos evaporíticos. Investigación y mitigación. In: Nisio S, Panetta S, Vita L (eds) Stato dell'arte sullo studio dei fenomeni di sinkholes e ruolo delle amministrazioni statali e locali nel gobernó del territorio. Apat-Dipartimento Difesa del Suolo, pp 367–378

Gutiérrez F, Arauzo T, Desir G (1993) Landslides in the Alfajarín gypsum escarpment. In: Gutiérrez M, Sancho C, Benito G (eds) Second European intensive course on applied geomorphology. Arid Regions, Zaragoza, pp 153–160

Gutiérrez F, Ortí F, Gutiérrez M, Pérez-González A, Benito G, Gracia J, Durán Valsero JJ (2001) The stratigraphical record and activity of evaporite dissolution subsidence in Spain. Carbonate Evaporite 16:46–70

Gutiérrez F, Lucha P, Guerrero J (2004a) La dolina de colapso de la casa azul de Calatayud (noviembre de 2003). Origen, efectos y pronóstico. In: Benito G, Díez Herrero A (eds) Riesgos naturales y antrópicos en Geomorfología. VII Reunión Nacional de Geomorfología, Toledo, pp 477–488

Gutiérrez F, Calaforra JM, Cardona F, Ortí F, Durán JJ, Garay P (2004b) El karst en las formaciones evaporíticas españolas. In: Andreo B, Durán JJ (eds) Investigaciones en sistemas kársticos españoles. IGME, Madrid, pp 49–87

Gutiérrez-Santolalla F, Gutiérrez-Elorza M, Marín C, Maldonado C, Younger PL (2005a) Subsidence hazard avoidance based on geomorphological mapping. The case study of the Ebro River valley mantled karst (NE Spain). Environ Geol 48:370–383

Gutiérrez-Santolalla F, Gutiérrez-Elorza M, Marín C, Desir G, Maldonado C (2005b) Spatial distribution, morphometry and activity of La Puebla de Alfindén sinkhole field in the Ebro River valley (NE Spain) applied aspects for hazard zonation. Environ Geol 48:360–369

Gutiérrez-Santolalla F, Acosta E, Ríos S, Guerrero J, Lucha P (2005c) Geomorphology and geochronology of sackung features (uphill-facing scarps) in the Central Spanish Pyrenees. Geomorphology 69:298–314

Gutiérrez F, Galve JP, Guerrero J, Lucha P, Cendrero A, Remondo J, Bonachea J, Gutiérrez M, Sánchez JA (2006) The origin, typology, spatial distribution, and detrimental effects of the sinkholes Developer in the alluvial evaporite karst of the Ebro River valley downstream Zaragoza city (NE Spain). Earth Surf Proc Landf 32:912–928

Gutiérrez M, Gutiérrez F (1998) Geomorphology of the tertiary gypsum formations in the Ebro Depression (Spain). Geoderma 87:1–29

Jones CJFP, Cooper AH (2005) Road construction over voids caused by active gypsum dissolution, with an example from Ripon, North Yorkshire, England. Environ Geol 48:384–394

Martínez JD, Johnson KS, Neal JT (1998) Sinkholes in evaporite rocks. Am Sci 86:38–51

McCalpin JP (1996) Field techniques in paleoseismology. In: McCalpin JP (ed) Paleoseismology. Academic Press, San Diego, pp 33–83

Ortí F, Salvany JM (1997) Continental evaporitic sedimentation in the Ebro basin during the Miocene. In: Busson G, Schreiber BCh (eds) Sedimentary deposition in Rift and Foreland basins in France and Spain. Columbia University Press, New York, pp 420–439

Quirantes J (1978) Estudio sedimentológico y estratigráfico del Terciario continental de los Monearos. Institución Fernando el Católico, C.S.I.C. Zaragoza, 200 pp

Remondo J, González A, Díaz de Terán JR, Cendrero A, Fabbri A, Cheng CF (2003) Validation of landslide susceptibility maps; examples and applications from a case study in Northern Spain. Nat Hazards 30:437–449

Sancho C, Peña JL, Lewis CJ, McDonald EV, Rhodes E (2004) Registros fluviales y glaciares cuaternarios en las cuencas de los ríos Cinca y Gállego (Pirineos y Depresión del Ebro), Geo-Guías. VI Congreso Geológico de España, Zaragoza, pp 181–205

Smith K (1996) Environmental hazards. Assessing risk and reducing disaster. Routledge, London, p 389

Soriano MA (1990) Geomorfología del sector centromeridional de la Depresión del Ebro. Institución Fernando el Católico, Zaragoza, 269

Soriano MA, Simón JL (1995) Alluvial dolines in the central Ebro Basin, Spain: spatial and environmental hazard analysis. Geomorphology 11:295–309

Torrescusa S, Klimowitz J (1990) Contribución al conocimiento de las evaporitas Miocenas (Fm. Zaragoza) de la Cuenca del Ebro, In: Ortí F, Salvany JM (eds) Formaciones evaporíticas de la Cuenca del Ebro y cadenas periféricas y de la zona de Levante. ENRESA-GPPG, Barcelona, pp 62–66

van Zuidam RA (1976) Geomorphological development of the Zaragoza region, Spain. Processes and landforms related to climatic changes in a large Mediterranean river basin. ITC, Enschede, 211 p
Waltham T, Bell F, Culshaw M (2005) Sinkholes and subsidence. Karst and cavernous rocks in engineering and construction. Springer, Chichester, p 382
Williams P (1972) Morphometric analysis of polygonal karst in New Guinea. Geol Soc Am Bull 83:761–796